



Contents lists available at ScienceDirect

Journal of Photochemistry & Photobiology, A: Chemistry

journal homepage: www.elsevier.com/locate/jphotochem

A selective turn-on fluorescent chemosensor 1,1-diaminoazine for azinphos-methyl

Monika Bhattu^a, Aabid A. Wani^b, Meenakshi Verma^a, P.V. Bharatam^b, Deepika Kathuria^{a,*}, Jesus Simal-Gandara^{c,*}^a University Center for Research and Development, Chandigarh University, Gharuan, Punjab 140413, India^b National Institute of Pharmaceutical Education and Research, Mohali, Punjab 160062, India^c Universidade de Vigo, Nutrition and Bromatology Group, Analytical Chemistry and Food Science Department, Faculty of Science, E32004 Ourense, Spain

ARTICLE INFO

Keywords:

Azinphos-methyl
Organophosphorus pesticide
1,1-diaminoazine
Nanoparticles
Turn-on fluorescence

ABSTRACT

Detection of organophosphorus pesticides (OPPs) is an important challenge in environmental chemistry, because their exposure to humans can cause severe health problems. In the current study, organic nanoparticles of (*E*)-(4-chlorophenyl)-1,1-diamino-2,3-diazabutadiene were developed using eco-friendly approach which was found to be in the range of 15–20 nm. These synthesized species exhibited both U.V. Visible and “turn-on” fluorescence responses in aqueous media for the selective detection of the extremely hazardous pesticide azinphos-methyl. These organic nanoparticles also exhibit a good linear relationship in the range of 1–100 μ M and the limit of detection (LOD) is 7.4 μ M. The selective fluorescence response was also observed in RO water, tap water and orange juice. The FT-IR and DFT studies helped in identifying the specific H-bonding interactions responsible for the selective detection of Azinphos-methyl.

1. Introduction

Pesticides are the organic chemical compounds which are used to kill the pests with an aim to increase the agricultural yield. Pesticides are applied as ground-based sprays to the agricultural land, allowing them to quickly reach surface-active agents, waterways, and other bodies of water.[1] The increased use of pesticides has led to the unavoidable environmental issues. Among all the pesticides, organophosphate pesticides (OPPs) are most commonly employed. The examples of OPPs (Fig. 1) include acephate (I), azinphos-methyl (II), chlorpyrifos (III), chlorpyrifosmethyl (IV), coumaphos (V), dichlorpos (VI), dicotophos (VII), ethoprophos (VIII), ethion (IX), fenitrothion (X), glycofosphate (XI), malathion (XII), parathion (XIII), parathion-methyl (XIV) and phosmet (XV). The general mode of action of OPPs in human body is the irreversible inhibition of acetylcholinesterase enzyme (AChE); a neurotransmitter. In humans, AChE is helpful in catalysing the hydrolysis of acetylcholine (ACh) into choline and acetic acid.[2] The irreversible inhibition of enzymatic activity leads to the accumulation of ACh at nerve junctions resulting into the nervous system disfunctioning. This may lead to convulsions, paralysis and even death. In case of environmental toxicity, the hydrolysis of OPPs leads to the formation of water

soluble components which persist in environment for a longer time.[3] Schemes 1 and 2.

Azinphos-methyl (II, O,O-Dimethyl-S-[(4-oxo-1,2,3-benzotriazin-3(4H)-yl)methyl]dithiophosphate) is most commonly employed OPP, generally used to prevent the growth of the annual grasses and various kinds of broad-leaved weeds, insects on various kinds of fruits.[4] It is also an important component in various marketed pesticidal formulations which include Gusathion, Crysthiron, Cotnion-methyl, Carfene, Guthion, Cotnion, Gusathion-M, R-1852, Bay 17,147 and Metriltrization.[5] Besides its usage, azinphos-methyl belongs to the extremely hazardous class of pesticides and it is considered as the most toxic OPP not only for humans but also for non targeted beneficial organisms. [6,7,8] Taking its increasing use and its toxicity into consideration, the eradication and detection of the azinphos-methyl has become an important concern. Conducting the literature survey on Scopus (accessed on 24/05/2022), it was observed that only few reports are there on the development of chemosensor for the detection of OPP. The literature survey for the detection of azinphos-methyl (Table 1) revealed that most of the reported methods includes liquid/gas chromatography with mass spectrometry[9], electrochemical,[10] capillary electrophoresis,[11,12,13] electrochemical liquid-phase microextraction,[14,11]

* Corresponding authors.

E-mail addresses: niperdeepika12@gmail.com (D. Kathuria), jsimal@uvigo.es (J. Simal-Gandara).<https://doi.org/10.1016/j.jphotochem.2022.114476>

Received 31 August 2022; Received in revised form 23 November 2022; Accepted 2 December 2022

Available online 6 December 2022

1010-6030/© 2022 The Author(s). Published by Elsevier B.V. This is an open access article under the CC BY license (<http://creativecommons.org/licenses/by/4.0/>).

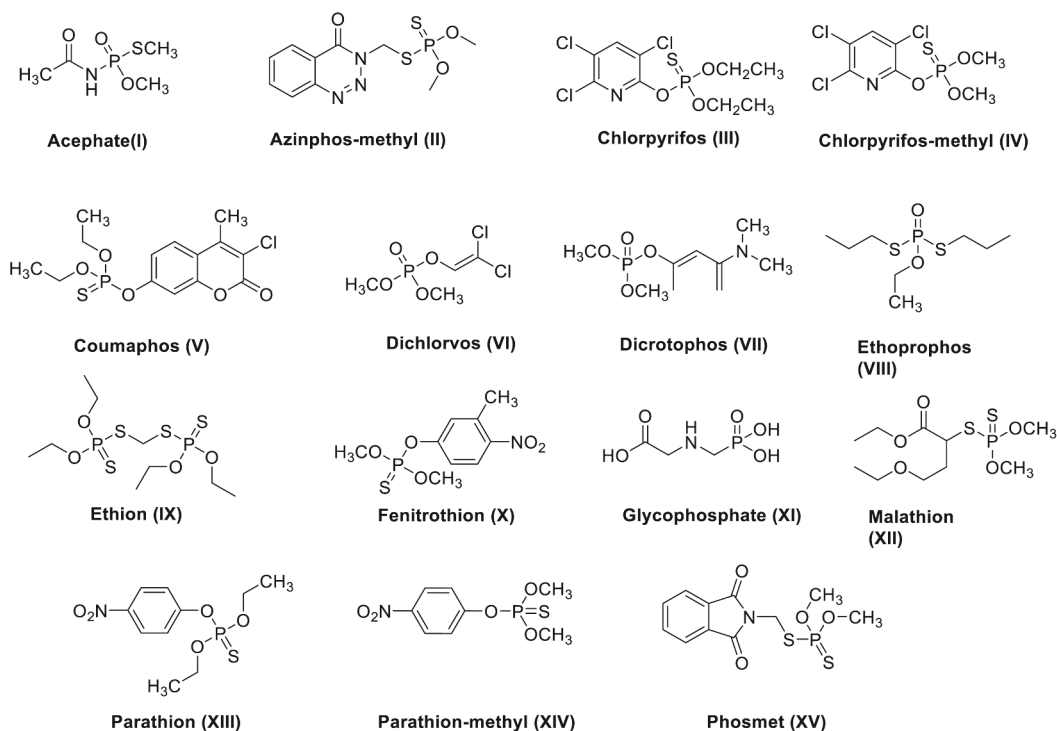
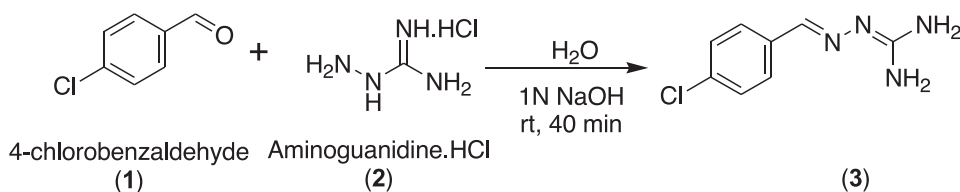
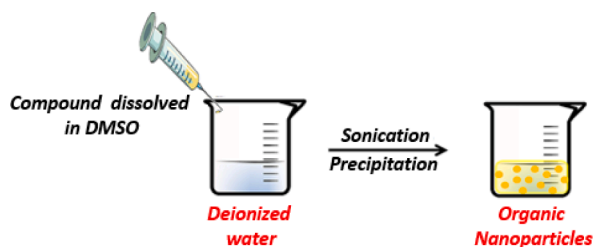


Fig. 1. Structure of important organophosphate pesticides (OPPs).



Scheme 1. Synthesis of (E)-(4-chlorophenyl)-1,1-diamino-2,3-diazabuta-1,3-diene.



Scheme 2. Schematic diagram for the synthesis of organic nanoparticles of 3.

flow injection spectrophotometric analysis,[15] and biosensors[16]. These methods possess various disadvantages which include i) time consuming analysis, ii) sample preparation, iii) high cost, and iv) trained personnel are required for operating the instruments and for the sample analysis. Among all the detection based techniques fluorescent based sensors are gaining scientific attention. Most of them belongs to enzyme based, metal based and only few of them belongs to organic scaffolds. [17,18] However, cost and toxicity of the developed receptor becomes a major concern.[19,20].

The limitations of the currently reported methods prompted us to develop a easily synthesizable and selective chemical sensors as an alternative to the available sensors.[30] For this purpose, 1,1-diaminoazine was selected. These scaffolds exhibit applications in medicinal chemistry, organic chemistry,[31] material chemistry,[32] structural

Table 1
Reported methods for the detection of azinphos-methyl.

S. No.	Detection technique	Matrix	Sensitivity	Reference
1	High Performance Liquid Chromatography	Water	11.9 ppb	Bushway <i>et al.</i> , 1982[21]
2	High Performance Liquid Chromatography (HPLC)	Soil	8.13 ng/mL	Sanchez <i>et al.</i> , 1992[22]
3	Gas Chromatography tandem mass spectrometry (GC-MS)	Water and apple juice	12.5 – 100 ppb	Kralj <i>et al.</i> , 2005[23]
4	Fluorescence Polarization Immunoassay	Water	0.150 mg/L	Tang <i>et al.</i> , 2008[24]
5	Optiqua MZI sensor	Water	0.2 mg/L	Tangena <i>et al.</i> , 2010[25]
6	ECL-ELISA	Vegetables	9.04 µg/L	Liu <i>et al.</i> , 2013 [26]
7	QuEChERS-GC/MS	Tomato	0.1 mg/kg	Domínguez <i>et al.</i> , 2014 [27]
8	HPLC-HRMS	Textile	5.0 ng/g	Hu <i>et al.</i> , 2017 [28]
9	Luminescence based on MOFs	Apple	16 ppb	Singha <i>et al.</i> , 2017[8]
10	Fluorescence	Water	1.73 nM	Kaur <i>et al.</i> , 2017[29]
11	Electrochemical	Water	2.964 µM	Erkmen <i>et al.</i> , 2020[1]

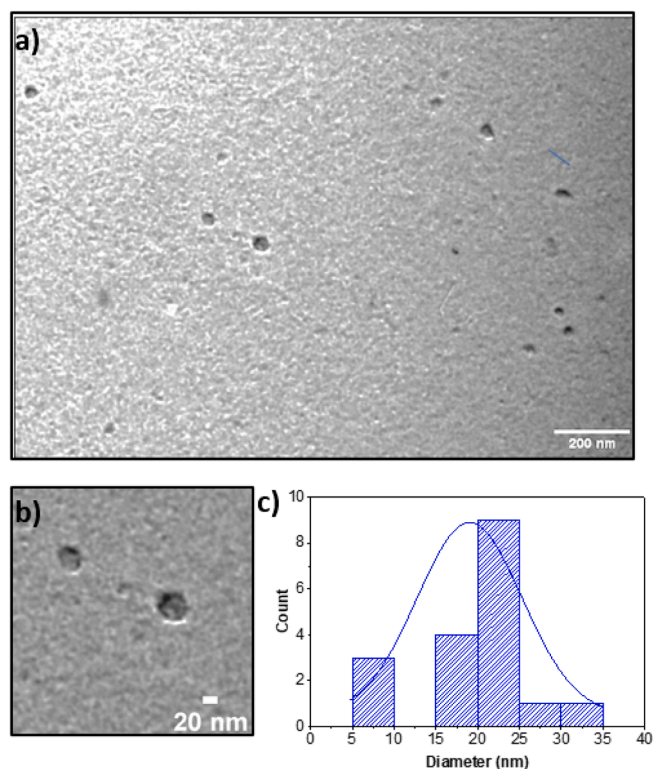


Fig. 2. Characterisation of ONPs of **3** using TEM: a) TEM image at resolutions of 200 nm; b) TEM image at resolutions of 20 nm; c) Size distribution curve and histogram of ONPs of **3** showing average size of nanoparticles lies between 15 and 20 nm.

chemistry, [3334] and as chemosensor. [35 36 37]. In most of the cases symmetrical azines were used, however, only limited reports suggest the use of unsymmetrical azines for the detection of pesticide which include the fluorescent turn on recognition of diethylchlorophosphate. [38] The structural features of azines such as H-bond accepting capacity, H-bond donating capacity and hydrophobicity motivated us to explore the applications of unsymmetrical azines as chemosensor and toxicity of pesticide, herein, we investigate the use of 1,1-diaminoazine for the selective detection of azinphos-methyl. In addition to the above facts, the use of azine as sensor offers various advantages such as i) ease in synthesis; ii) eco-friendly approach; and iii) easily available starting material (aldehydes).

2. Experimental section

2.1. Materials and instruments

Analytical grade chemicals named sodium hydroxide, aminoguanidine.HCl, 4-chlorobenzaldehyde and pesticide standards (100 mg/L, including glyphosphate, imidacloprid, phosmet, azinphos-methyl, ethion and chlorpyrifos) were purchased from Sigma-Aldrich. Water samples were collected from the laboratory. Orange juice was taken by grinding the oranges procured from local market. Shimadzu fluorescence spectrophotometer was used to measure fluorescence (RF-6000). UV studies were carried out using the Shimadzu UV-Visible Spectrophotometer (UV-vis 2600). Transmission electron microscopy (TEM) studies were performed using JEM-1400 instrument having an accelerating voltage of 200 kV (JEOL, Japan). Dynamic Light Scattering and Zeta potential was obtained on Malvern zeta size analyzer. The quantum chemical calculations were carried out using the Gaussian 09 suite of programs. Geometry optimization of compounds was performed by DFT using B3LYP method. The basis set used was 6-311 + G(d,P) for C,H,N, O, Cl. The frequency calculations were carried out on all the structures to

verify character of stationary points (minima v/s saddle point).

2.2. Synthesis of organic compound and its nanoparticles

2.2.1. Synthesis of (E)-(4-chlorophenyl)-1,1-diamino-2,3-diazabuta-1,3-diene (**3**)

For the synthesis of azines, 2 mL aqueous sodium hydroxide solution was added to a mixture of 4-chlorobenzaldehyde (**1**) and aminoguanidine (**2**) hydrochloride in aqueous medium and the reaction mixture was stirred at room temperature until the precipitates got formed. The obtained precipitates were filtered and dried to get the final precipitates. [32] The synthesized product was further characterized using the ^1H NMR, ^{13}C NMR and mass spectrometry. Off-White solid (139 mg, 99 %); ^1H NMR (400 MHz, DMSO- d_6) δ 7.97 (s, 1H), 7.70 (d, J = 8.5 Hz, 2H), 7.37 (d, J = 8.4 Hz, 2H), 5.95 (br s, 2H), 5.53 (br s, 2H). ^{13}C NMR (101 MHz, DMSO- d_6) δ 161.3, 142.0, 136.5, 132.2, 128.8, 128.2; HRMS (ESI-TOF) m/z : [M + H]⁺ Calcd for $\text{C}_8\text{H}_{10}\text{ClN}_4$ 197.0584; Found 197.0587 (See Supporting Information, Figs. S1-S3).

2.2.2. Preparation of organic nanoparticles

The sensing properties of the synthesized compound was explored by processing them into the organic nanoparticles (ONPs). For the preparation of ONPs, re-precipitation method has been utilized. [39] For this purpose, 5 mM solution of the synthesized compound was prepared by dissolving the 1 mg of the compound 1 mL of DMSO. The prepared solution was further injected in the form of small aliquots into 100 mL of milli Q water to get the final concentration of 50 μM . The addition was done using a microsyringe in a time span of 30 min under ultrasonication conditions. The sonication was continued for 15 more minutes. The characterisation of the prepared ONPs was done using TEM in order to find the size of prepared nanoparticles (NPs). The synthesized nanoparticles were characterized using the TEM analysis (Fig. 2a and b) and the average size distribution curve was plotted (Fig. 2c). The average size of the particles was found to be 15–20 nm.

2.3. Photophysical studies

UV-Visible absorption and fluorescence emission spectral studies were carried out for estimating the recognition behaviour of the prepared nanostructures. For carrying out the recognition studies, solution of heavy metals (5 mM) and pesticides (5 mM) were prepared. These prepared solutions (100 μL) were added to the 5 mL of host ONPs solutions. Firstly, the UV absorption spectra of the pure ONPs were recorded and then spectra of the prepared solutions (100 μL toxin + 5 mL ONPs) were taken after 20 mins of addition. If the absorbance response shows change (increase/decrease/shift) with any of the particular toxin then further studies such as titration studies, competitive studies, effect of environmental conditions and real time sample analysis were performed in order to find out the selectivity and sensitivity of the host sensor towards that specific toxin. The titration studies were performed by subsequent addition (0–100 μM) of the specific toxin to the ONPs (5 mL, 25 μM). The spectra was recorded after each addition in order to find the linear response of the sensor. The limit of detection (LOD) was calculated using the 3σ method. [40] The interference study was performed by analysing the developed sensor response with that specific toxin in presence of other similar competing toxins. Further, the stability of the sensor has been investigated at a pH range of 3–12. The real sample analysis was performed in water and orange juice by spiking the sample with known concentration of toxin and further recovery was calculated.

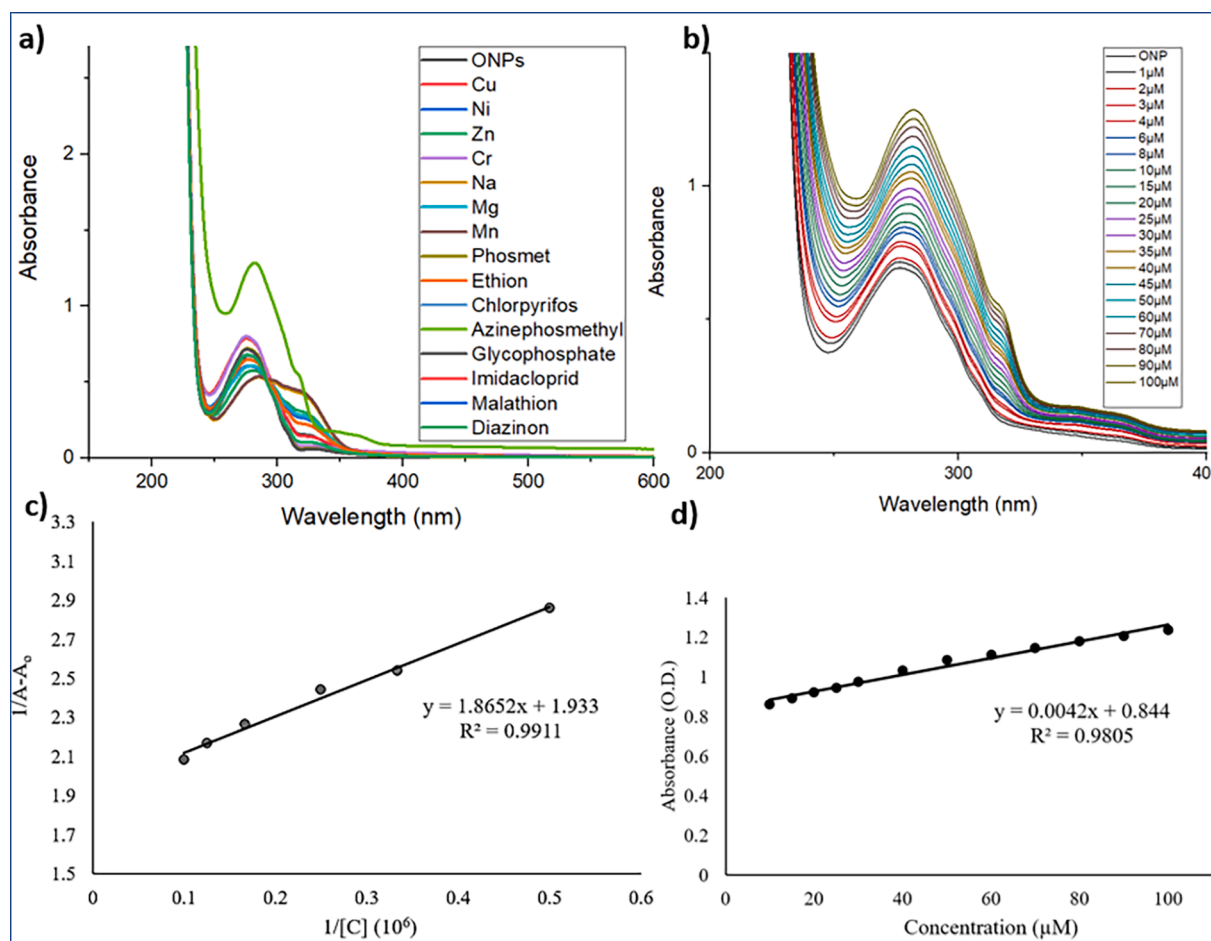


Fig. 3. A) UV-Visible Spectra of host ONPs in presence of various OPPs and metal cations at 100 μM concentration. B) U.V. titration studies of host ONPs with azinphos-methyl (1–100 μM). C) B-H Plot of absorption spectra of host ONPs after addition of azinphos-methyl. D) Linear curve of host ONPs with increasing concentration of azinphos-methyl (10–100 μM).

3. Results and discussion

3.1. Synthesis of (E)-(4-chlorophenyl)-1,1-diamino-2,3-diazabuta-1,3-diene and its ONPs

For the synthesis of azines, 2 mL aqueous sodium hydroxide solution was added to a mixture of 4-chloro benzaldehyde (1) and amino-guanidine hydrochloride (2) in water and the reaction mixture was stirred for 40 min. at ambient temperature (25–30 $^{\circ}\text{C}$) until the precipitates got formed. The obtained precipitates were filtered and dried to get the off-white precipitates in 93 % yield. The characterization of the synthesized compound was carried out using ^1H NMR, ^{13}C NMR, and HRMS spectrometry.

Further, the ONPs of **3** were prepared using reprecipitation method for which 1 mg of the **3** was dissolved in 1 mL of DMSO and was further injected in 99 mL of mill Q water using microsyringe. The addition was done under continuous sonication and after the complete addition the solution was kept under sonication for further 15 min. The synthesized ONPs were characterized using TEM.

3.2. UV-Visible spectroscopy studies

3.2.1. Recognition study

Absorption spectroscopy was employed for carrying out the recognition studies. The ONPs of synthesized compound (**3**) were screened against various organophosphate pesticides (OPPs) such as azinphos-methyl, chlorpyrifos, ethion, phosmet, glycofosphate and

chlorpyrifos methyl and metal ions such as Cu^{2+} , Ni^{2+} , Zn^{2+} , Cr^{2+} , Na^+ , Mg^{2+} , and Mn^{2+} and their UV spectra was recorded. For analysing the selectivity, 5 mL of 25 μM solution of ONPs were treated with the 100 μL aqueous solution (5 mM) of aforementioned metal ions and OPPs. UV-vis absorption spectroscopic studies were carried out using the quartz cuvettes having 1 cm pathlength at room temperature. The absorption response of the host ONPs shows a maxima at a wavelength of 275 nm. All the screened OPPs and metal cations showed negligible change except azinphos-methyl. A hyperchromic shift in the absorption spectra was observed in presence of azinphos-methyl which was $\lambda^{\text{max}} = 275$ nm (Fig. 3a). The shift indicates the selective binding of the ONPs towards azinphos-methyl and is attributed towards the change in the electron density of host ONPs.

3.2.2. Titration study of host ONPs with azinphos-methyl

After conducting the binding studies, the efficacy of the host ONPs towards azinphos-methyl was measured by adding the rising concentration of the OPPs and their effect on the absorptive curve was monitored. These studies were carried out by the subsequent addition of the 20 equivalents (1 μL -100 μL) of azinphos-methyl (5 mM) to the 5 mL of host ONPs solution (25 μM). Thus, the titration studies were performed over a concentration range of 1 μM to 100 μM . The absorptive response of the host ONPs exhibits a hyperchromic shift on introduction of the azinphos-methyl (Fig. 3b) indicating the electron density transfer between the host and guest molecules.

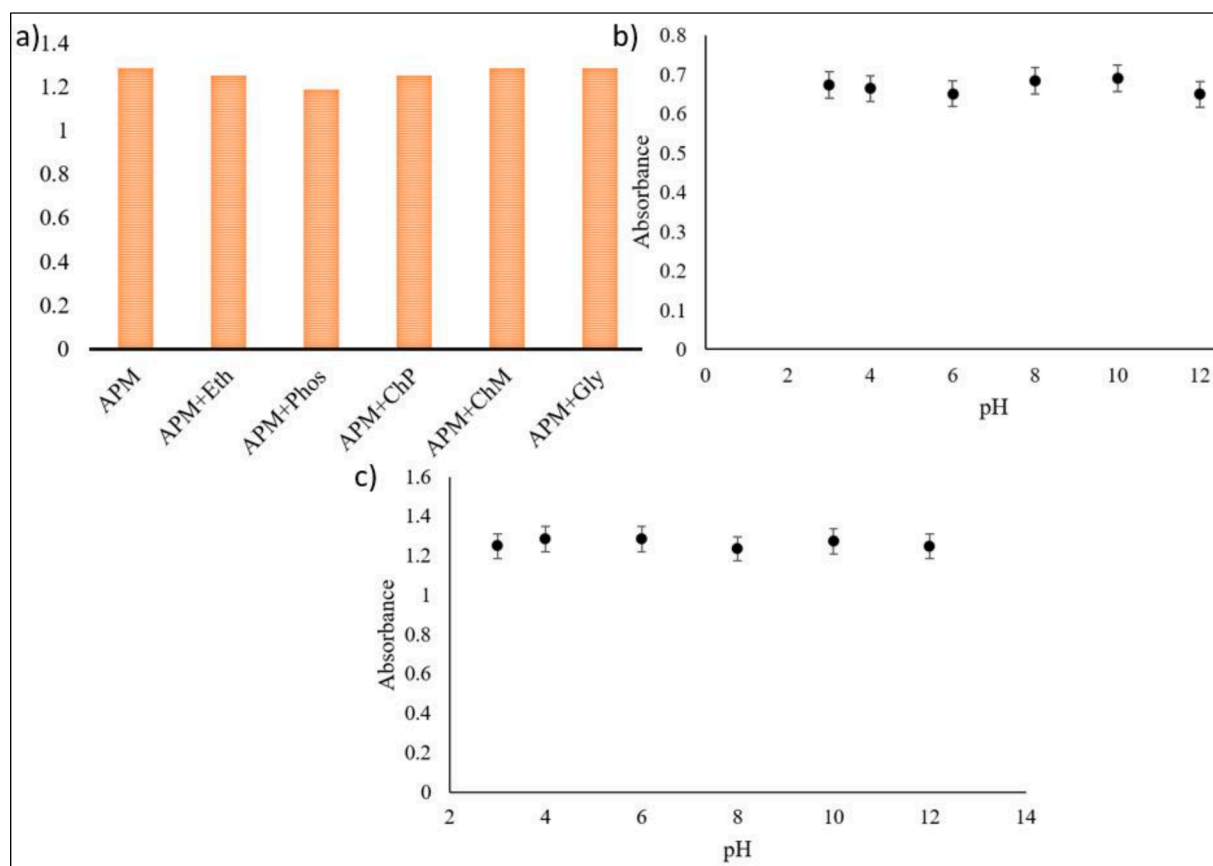


Fig. 4. a) Interference studies of the host ONPs towards azinphos-methyl in presence of competing OPPs by UV spectrophotometer. Where, APM stands for Azinphos-methyl; Eth for ethion; Phos for phosmet; ChP for chlorpyrifos; ChM chlorpyrifos-methyl; Gly for glyphosate; b) Effect of pH on absorbance of ONPs; and c) Complex (ONPs + Azinphos-methyl, c).

3.2.3. Association constant (K_a) and limit of detection (LOD)

Benesi and Hildebrand's graphical strategy (B-H plot) was employed to measure the binding efficacy of the host (ONPs) and guest (azinephos-methyl) molecules. The binding efficacy was calculated in terms of association constant by taking the slope and intercept of B-H plot into consideration (Fig. 3c). The association constant was found to be $1.03 \times 10^6 \text{ M}^{-1}$.

Further the limit of detection was calculated in order to confirm the high sensitivity and affinity of the host ONPs towards the azinphos-methyl. The LOD was calculated by plotting the graph of absorbance (y-axis) at wavelength 275 nm against concentration (μM) of guest (x-axis) (Fig. 3d). The LOD was calculated using 3σ and was found to be $2.18 \mu\text{M}$.

3.2.4. Interference study

Interference studies were carried out by mixing 100 μL solutions (5 mM) of several OPPs such as chlorpyrifos, ethion, phosmet, glyco-phosphate and chlorpyrifos methyl into the host-guest solution. The UV-Visible spectrum was recorded after the sequential addition of the solution of each OPP. As seen in Fig. 4a, no considerable interference was found in the absorption spectra of ONP-azinphosmethyl in presence of other interfering OPPs (ethion, phosmet, chlorpyrifos, chlorpyrifosmethyl glyco-phosphate) suggesting the high selectivity of host ONPs towards the azinephos-methyl. Further, the effect of pH has been studied by increasing and decreasing the pH value using 1 N NaOH and 1 N HCl. The proposed sensor was found to be stable at a pH range of 3–12 in absence and presence of azinphosmethyl. (Fig. 4b and c).

3.3. Fluorescence spectroscopic studies of ONPs with pesticide

Further, the fluorescence studies were carried out by taking the excitation wavelength of 275 nm and the host ONPs were screened against various kinds of OPPs as well as metal ions such as metal ions such as Cu^{2+} , Ni^{2+} , Zn^{2+} , Cr^{2+} , Na^+ , Mg^{2+} , and Mn^{2+} . A considerable increase in the emission spectra was observed for the azinphos-methyl and no change was observed for other organophosphate pesticides signifies the excellent specificity and selectivity towards azinphos-methyl in aqueous solutions (Fig. 5a). Further, in order to find the selectivity and sensitivity of the host ONPs towards the azinphos-methyl, further studies such as titration studies, competitive studies, environmental effects and real sample analysis were also performed.

To find out the sensitivity of host ONPs towards azine phomethyl, the effect of the various concentrations of guest OPP was monitored on the emission spectra of the host ONPs. For this purpose, subsequent addition of 20 equivalents (1 μL -100 μL) of azinphos-methyl (5 mM) was done in the 5 mL of 25 μM ONPs solution. The emission spectra of the solution was observed after each consequent addition. The emission spectra showed an increase in the fluorescence intensity of the spectra with increasing concentration (Fig. 5b). The linear regression plot was taken by plotting the graph of fluorescence intensity (y-axis) against [Q] (x-axis) at the emission maxima i.e. 355 nm (Fig. 5c). The LOD of the host ONPs towards the azinphos-methyl was calculated using the linear regression plot. The LOD was found to be $7.4 \mu\text{M}$.

Furthermore, in order to understand the maximum binding efficacy of azinphos-methyl to ONPs, fluorescence Job's plot was analysed. [41] For this purpose, the molar ratio of the azinphos-methyl (25 μM) and ONPs (25 μM) were varied gradually. At different ratios of receptor: target, different kinds of interactions were observed between the

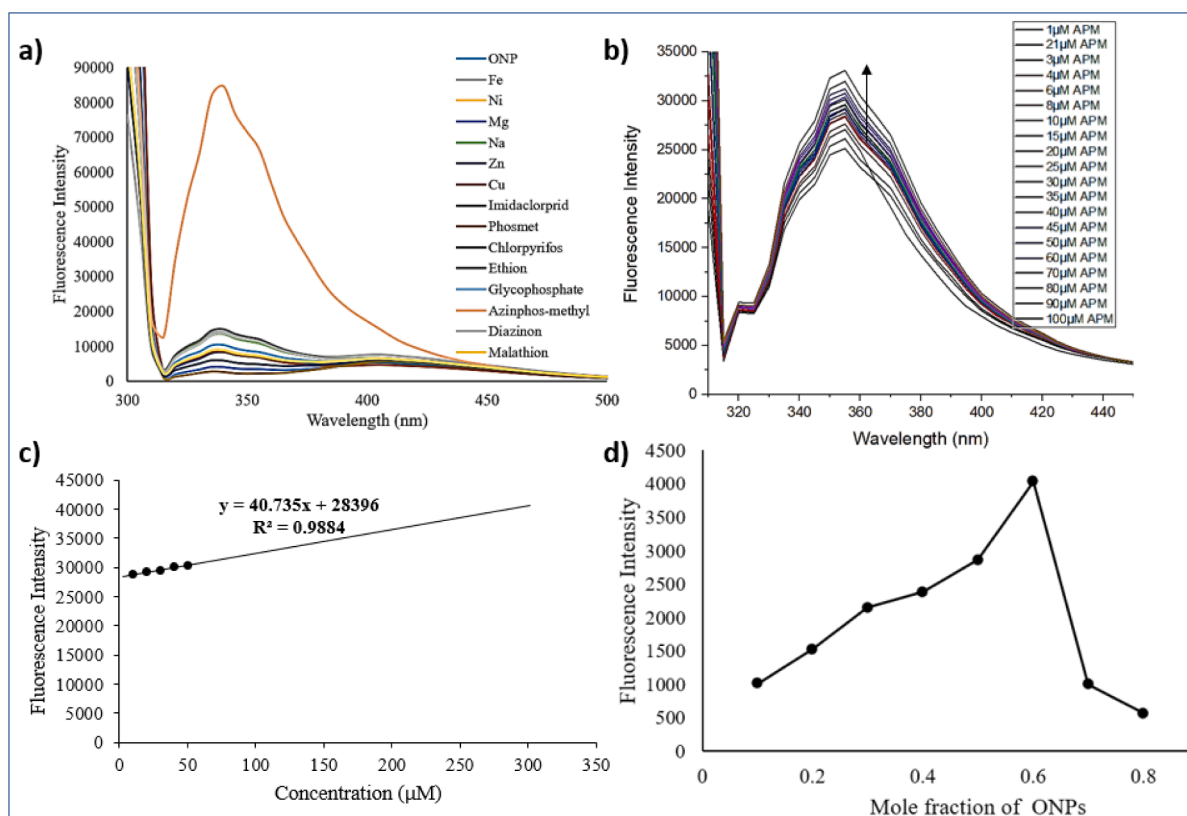


Fig. 5. A) binding studies of host onps (50 μM) for various kinds of OPPs and metal ions at 100 μM concentration. b) Fluorescence titration studies of host ONPs by adding azinphos-methyl (1 μM -100 μM) c) Linear Plot of host ONPs binding with azinphos-methyl; d) Job's plot by varying the molar ratio of ONPs:Azinphos-methyl from 0.1:0.9 to 0.9:0.1.

receptor and target molecule. The maximum fluorescence intensity were observed at molar ratio of 0.4:0.6 (ONPs:Azinphos-methyl) which suggests 1:1 stoichiometry of ONPs:Azinphos-methyl (Fig. 5d).

Further, the interference studies were carried out by subsequently adding the potential OPPs (100 μL of 5 mM OPP) to a solution of host ONPs and guest azinphos-methyl. No considerable change has been observed in the emission spectra of the ONPs-azinphos-methyl in presence of these potential competing OPPs indicating the high selectivity of host ONPs against azinphos-methyl (Fig. 6a). The effect of pH was studied over a wide pH range and was found to be stable over a pH range of 5–9 in absence and presence of azinphos-methyl (Fig. 6b and c).

4. Plausible mechanism for detection of azinphosmethyl

Fluorescence properties of the 1,1 diamino azines were investigated in water as solvent by exciting the ONPs at 275 nm and the emission was observed at 400 nm due to the donating efficacy of the 1,1 diamino group and the accepting efficacy of the iminic group. Various factors contributes in the change in the emissive properties of these azinic frame which includes a) nature of substituents (EWG/EDG) attached to the azine frame b) concentration of receptor molecule; and c) concentration of analyte. Based on the nature of substituent, the azine can behave as conjugation stopper or switcher. Owing to the low concentration of azine molecules in ONPs solution, the intermolecular interactions between receptor/azine molecules ($-\text{C}=\text{N}-\text{N}=\text{C}-$) were very less and thus the molecules were free to undergo rotation across $\text{N}-\text{N}$ bond. Hence, the excitation energy required for emission was utilised for rotation which results in the restoration of the receptor to ground state via a non radiative pathway. The addition of azinphosmethyl (analyte) to the ONPs solution (1,1-diaminoazine frame) leads to the formation of hydrogen bond between the ONPs and molecules of analyte. This interaction may restricts the free rotation across $\text{N}-\text{N}$ bond. [42,43] The

restriction may lead to the increase the fluorescence emission of the complex formed which were further confirmed by FT-IR and TD-DFT studies.

5. Mechanistic support

5.1. Computational study

From the above experimental work, it can be concluded that there is a clear complex formation which is responsible for the observed enhancement in the fluorescence. To explore the possible 3D structure of complex which is responsible for the observed fluorescence, quantum chemical calculations were carried out using Gaussian 09 package. [44,45] Geometry optimizations were performed by density functional theory (DFT) B3LYP/6-311 + G(d,p) level. Initially, it was thought a rigid molecular environment is formed due to $\text{N}-\text{P}$ bond formation. Structure A represents the possible product with $\text{N}-\text{P}$ covalent bond. The free energy change for the formation of A has been estimated to be 28.93 kcal/mol endergonic. Considering this value is very high and also considering that involves a large energy requirement, the formation of complex A is not practical and thus attempts were made to identify the 3D-structures of complexes which involve only associative interactions. Four different possibilities each with strong intramolecular H-bonds have been considered. They are labelled as **4a**, **4b** and **5a**, **5b**. **4a** and **4b** carry H-bond interactions between $-(\text{CNH}_2)_2$ group and the **II** (2H-bonds each). The complexes **5a** and **5b** carry the interactions between $\text{CH}=\text{N}=\text{N}=\text{CNH}_2$ unit of azine and **II** (3H-bonds each). The energy required for the formation of these four complexes are 1.31, 1.41, 3.640 and 3.645 kcal/mol respectively, all are marginally endergonic (coordinates of the complexes are given in SI). Therefore, among them **4a** was found to be most stable complex. The 3D-structures of all the four complexes are provided in Fig. 7. The next step of the quantum chemical analysis is

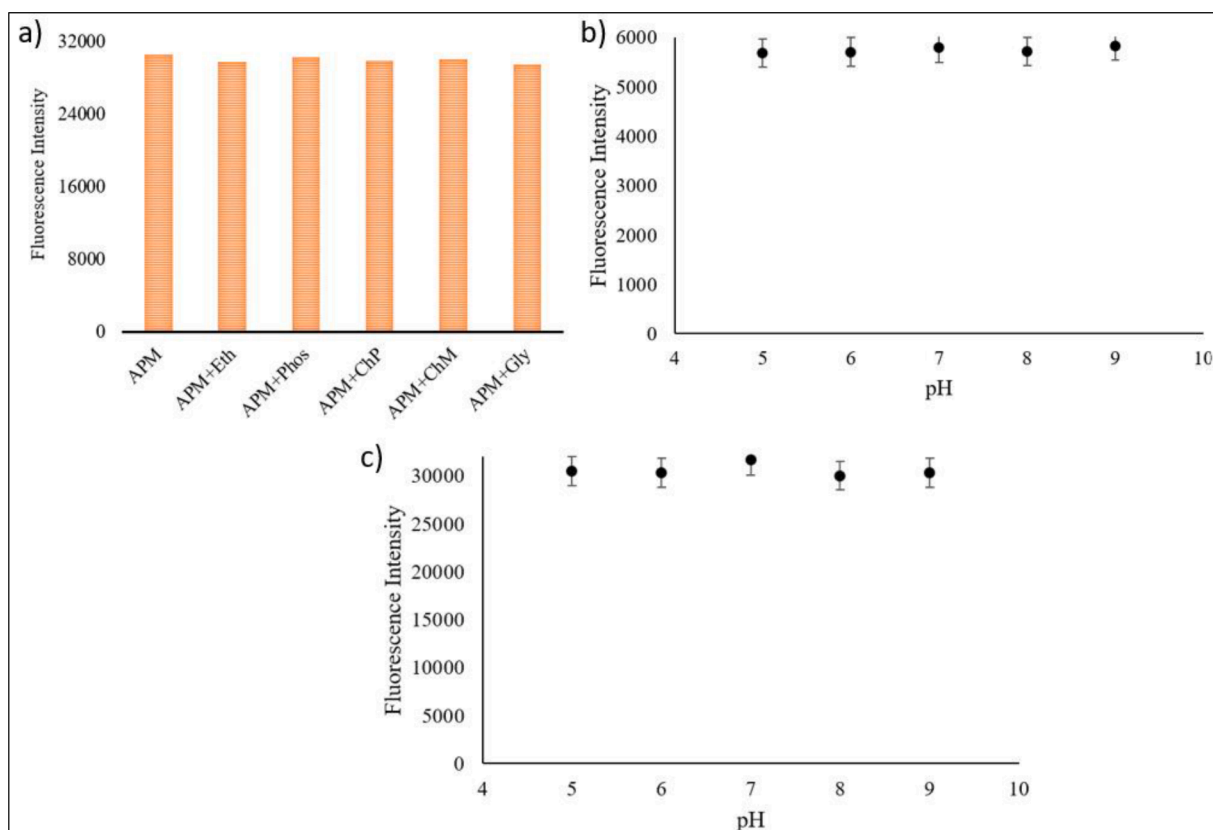


Fig. 6. A) fluorescence interference studies of the host onps towards azinphos-methyl in presence of competing opps. where, apm stands for azinphos-methyl; eth for ethion; phos for phosmet; chp for chlorpyrifos; chm chlorpyrifos-methyl; gly for glyphosate; b and c) effect of pH on fluorescence intensity of the onps (b); and onps + Azinphos-methyl complex (c).

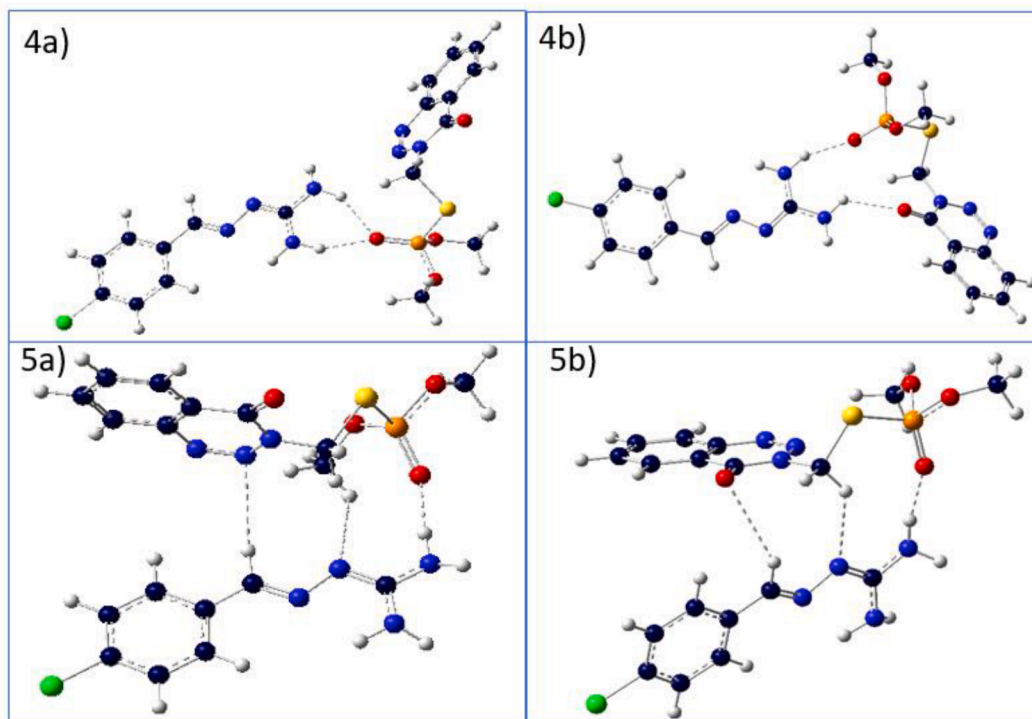


Fig. 7. Representation of 3D structures of possible complexes (4a, 4b, 5a and 5b) of receptor 3 with azinphos-methyl (II).

Table 2
TD-DFT results for complex-4a, 4b, 5a, 5b and Azinphos-methyl.

S. No.	Complex	HOMO-LUMO (eV)
1	complex-4a	4.7507
2	complex-4b	4.9706
3	complex-5a	5.4790
4	complex-5b	5.6278
5	Azinphos-methyl	6.5417

to perform TD-DFT calculations to estimate the excitation energies and associated λ^{\max} values. The estimated λ^{\max} values have been compared with experimental results. To gain the confidence in the ability of quantum chemical methods in estimating the λ^{\max} values, the experimental λ^{\max} values of II (208 nm) have been compared with that of the calculated value (207 nm). Further, the HOMO-LUMO energy difference values (ΔE , Table 2) were estimated which was found to be 4.75 eV, 4.97 eV, 5.47 eV and 5.62 eV for complex 4a, 4b, 5a and 5b respectively. The lowest HOMO-LUMO gap of 4a complex suggest that the associative interactions of 4a may attribute towards the enhancement in the fluorescence. The contour maps of the molecular orbitals are provided in Fig. 8. Many other alternative 3D-structures were also considered, but

ignored because of very high ΔG values. Generally, it is known that any compound exhibits fluorescence when it enters into rigid molecular environment and this increase in rigidity increases the observed fluorescence in complex. The observed rigidity is very clear in all the complexes. Also π stacking interactions may get triggered after the initial hydrogen bond formation (Friedlands book, Biophysical methods) Fig. 9.

5.2. Fourier transform infrared (FT-IR) analysis

The formation of complex (4a) via H-bonding was further confirmed by FTIR studies by comparing FTIR spectra of receptor, complex and pure azinphos-methyl (reference). The comparison studies show origination of new peaks and shift in the already existing peaks in spectra of complex in comparison to the pure azinphos-methyl which indicates the interaction of azinphosmethyl with the receptor molecule. The receptor molecule exhibit transmittance at 2993 cm^{-1} corresponds to N—H stretching. However, complex shows transmittance at 3065 cm^{-1} corresponding to the N—H stretching ($\text{N—H}\cdots\text{S}=\text{P}$). The shift in the peak was observed owing to the stretching of the N—H bond due to its participation in H-bonding. A high intensity peak at 3463 cm^{-1} corresponding to H-bonding of the receptor molecule with target azinphos-

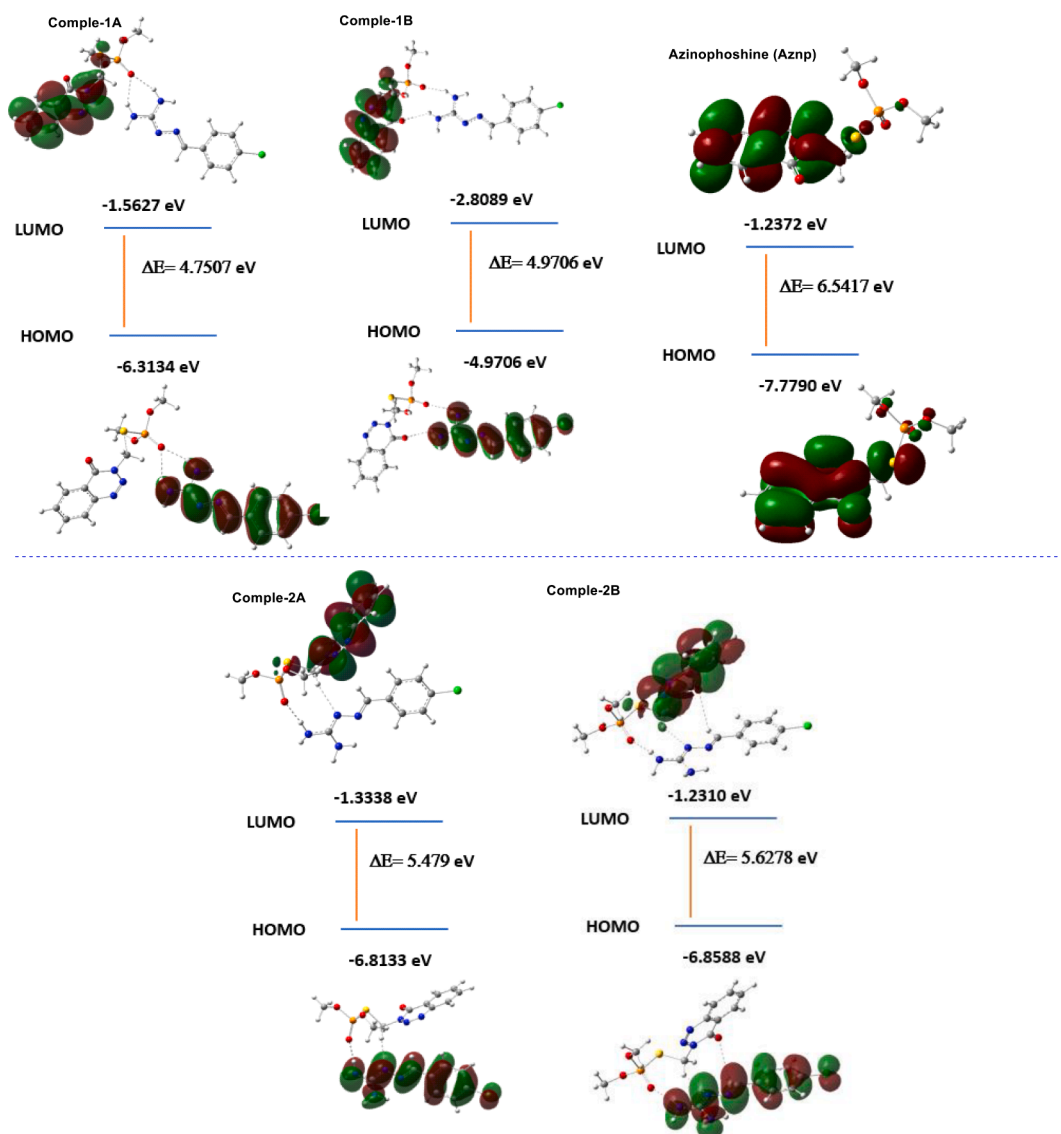


Fig. 8. HOMO – LUMO orbitals of complexes and Azinphos-methyl (II).

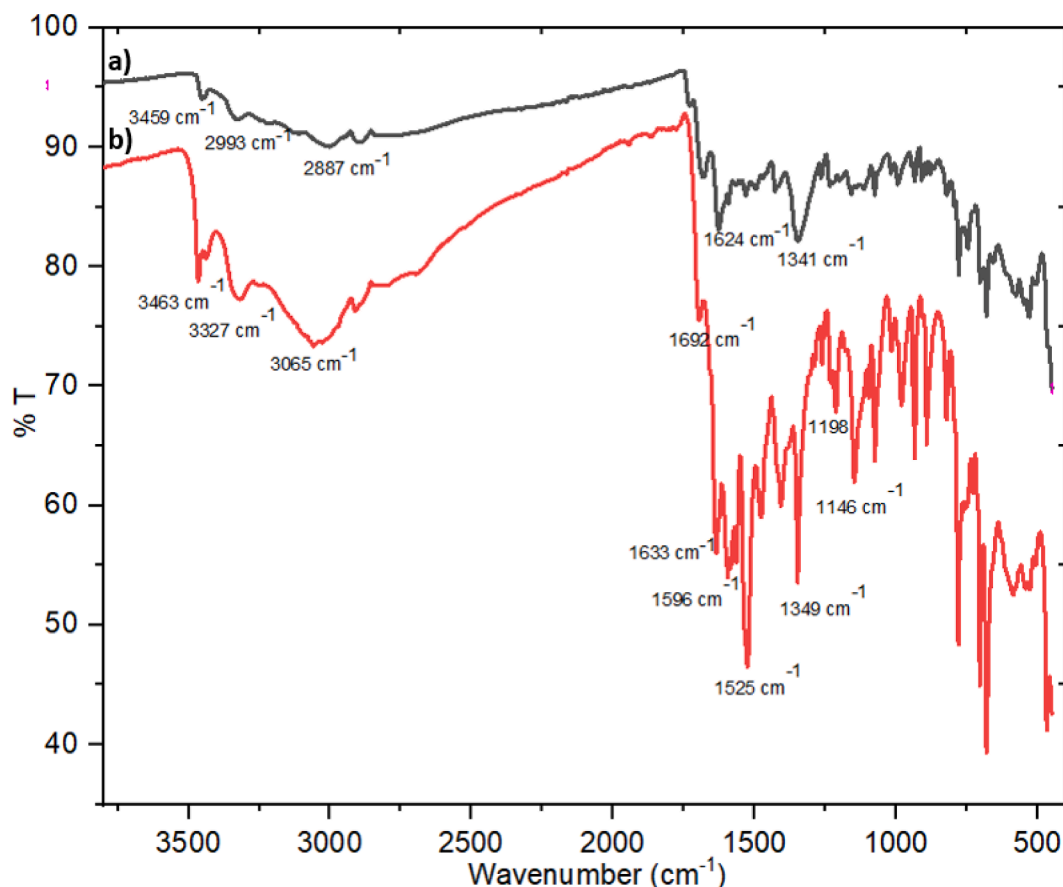


Fig. 9. FTIR spectra of a) receptor (ONPs); and b) complex receptor + target (azinphos-methyl).

Table 3

Real sample analysis of artificially prepared samples of azinphos-methyl containing water and juice samples and their percentage recovery using proposed sensor.

S. No	Sample	Spiked Concentration	Concentration Found	% Recovery
1	S-1	25 μM	22.14 μM	88.86 %
2	S-2	15 μM	13.06 μM	88.56 %
3	S-3	10 μM	8.84 μM	88.4 %
4	J-1	25 μM	22.97 μM	91.88 %
5	J-2	50 μM	44.51 μM	89.02 %
6	RO-1	25 μM	24.43 μM	97.72 %
7	RO-2	50 μM	48.15 μM	96.3 %
8	DW-1	25 μM	24.91 μM	99.64 %
9	DW-1	50 μM	49.46 μM	98.92 %

methyl. In figure a and b, the peak at 1624 cm^{-1} and 1633 cm^{-1} shows the C=N stretching which confirms no participation of the iminic nitrogen in complex formation.

6. Real sample analysis

To determine the applicability of the synthesized sensor in the real samples, water (tap Water, RO water and distilled water) and orange juice samples were taken. The water samples were taken as such. For preparing the juice sample, the oranges were procured from local market and blended to obtain the sample. Initially, the samples were analysed for the detection of azinphos methyl and the analysis signifies the absence of the pesticide. Further the samples were spiked with a known concentration of azinphos methyl by adding the 10 μL , 20 μL , 25 μL and 50 μL of azinphos-methyl (5 mM) in 5 mL of aforementioned samples and the final concentration of azinphos-methyl in spiked samples was

10 μM , 20 μM , 25 μM and 50 μM , respectively. The analysis was performed in order to find out the concentration and recovery of the spiked pesticide (Table 3).

The results showed that the proposed sensor had a 88-99 percent accuracy and could measure azinphos methyl even at low level of concentrations (μM).

7. Conclusions

Azinphos-methyl is a pesticide, which also exhibits nerve agent characteristics and thus is highly dangerous, its detection in aqueous media has been a challenge. In the current study, a facile synthesis of (*E*)-(4-chlorophenyl)-1,1-diamino-2,3-diazabutadiene was achieved using reported method. The nanoparticles of this species were developed using re-precipitation (DMSO) method and were characterised using TEM analysis which showed the average size of ONPs varies from 15 to 20 nm. These particles were employed for the detection of metals successfully, but the selectivity was not sufficiently high. Further, these particles were employed for the OPP detection. The results indicated that these organic nanoparticles are highly efficient in selectively detecting the pesticide azinphos-methyl. This is due to the formation of a complex between the sensor and the pesticide, the 3D structural details of the complex have been understood by performing quantum chemical analysis. The association constant ($1.03 \times 10^6\text{ M}^{-1}$) between the sensor and the pesticide has been determined with the help of UV-Visible spectroscopy. The strong binding constant ($\log K_a = 5.92$) of this sensor indicate efficient interaction with the pesticide. The “turn on” property of the sensor was identified with the help of UV-visible and fluorescence spectral analyses. The 1,1-diaminoazine based sensor has shown several advantages over existing sensors reported for azinphos-methyl detection viz. (i) Greener approach-based synthesis (ii) strong turn on fluorescence

response in aqueous solution (iii) least interference by other pesticides for the recognition of azinphos-methyl. The limit of detection for the sensor was found to be 7.4 μM which is far lower than the minimum toxicity dosage/day.

CRedit authorship contribution statement

Monika Bhattu: Data curation, Formal analysis, Methodology, Validation. **Aabid A. Wani:** Investigation, Data curation, Software. **Meenakshi Verma:** Resources. **P.V. Bharatam:** Conceptualization, Formal analysis, Visualization, Supervision. **Deepika Kathuria:** Investigation, Funding acquisition, Methodology, Supervision. **Jesus Simal-Gandara:** Investigation, Conceptualization, Formal analysis, Funding acquisition, Methodology, Visualization.

Declaration of Competing Interest

The authors declare that they have no known competing financial interests or personal relationships that could have appeared to influence the work reported in this paper

Data availability

Data will be made available on request.

Acknowledgements

D.K. thanks financial support from Department of Science and Technology, New-Delhi, India (Grant no.: SP/YO/2021/2314) for providing a funding.

Funding for open access charge: Universidade de Vigo/CISUG.

Appendix A. Supplementary data

Supplementary data to this article can be found online at <https://doi.org/10.1016/j.jphotochem.2022.114476>.

References

- [1] C. Erkmen, S. Kurbanoglu, B. Uslu, Fabrication of poly(3,4-ethylenedioxythiophene)-iridium oxide nanocomposite based Tyrosinase biosensor for the dual detection of catechol and azinphos methyl, *Sensors Actuators, B Chem.* 316 (2020) 128121, <https://doi.org/10.1016/j.snb.2020.128121>.
- [2] M. Bhattu, M. Verma, D. Kathuria, Recent advancements in the detection of organophosphate pesticides: A review, *Recent advancements in the detection of organophosphate pesticides: A review* 13 (38) (2021) 4390–4428.
- [3] H. Kojima, S. Takeuchi, T. Nagai, Endocrine-disrupting potential of pesticides via nuclear receptors and Aryl hydrocarbon receptor, *J. Heal. Sci.* 56 (2010) 374–386, <https://doi.org/10.1248/jhs.56.374>.
- [4] S. Buono, S. Manzo, G. Maria, G. Sansone, Toxic effects of pentachlorophenol, azinphos-methyl and chlorpyrifos on the development of *Paracentrotus lividus* embryos, *Ecotoxicology.* 21 (2012) 688–697, <https://doi.org/10.1007/s10646-011-0827-6>.
- [5] M.E. Sierszen, S.J. Lozano, Zooplankton population and community responses to the pesticide azinphos-methyl in freshwater littoral enclosures, *Environ. Toxicol. Chem.* 17 (1998) 907–914, [https://doi.org/10.1897/1551-5028\(1998\)017<0907:ZPACRT>2.3.CO;2](https://doi.org/10.1897/1551-5028(1998)017<0907:ZPACRT>2.3.CO;2).
- [6] C.G. Flocco, M.P. Carranza, L.G. Carvajal, R.M. Loewy, A.M. Pechén De D'Angelo, A.M. Giulietti, Removal of azinphos methyl by alfalfa plants (*Medicago sativa* L.) in a soil-free system, *Sci. Total Environ.* 327 (2004) 31–39, <https://doi.org/10.1016/j.scitotenv.2003.08.024>.
- [7] S.O. Obare, C. De, W. Guo, T.L. Haywood, T.A. Samuels, C.P. Adams, N.O. Masika, D.H. Murray, G.A. Anderson, K. Campbell, K. Fletcher, Fluorescent chemosensors for toxic organophosphorus pesticides: a review, *Sensors.* 10 (7) (2010) 7018–7043.
- [8] D.K. Singha, P. Majee, S.K. Mondal, P. Mahata, Highly Selective Aqueous Phase Detection of Azinphos-Methyl Pesticide in ppb Level Using a Cage-Connected 3D MOF, *ChemistrySelect.* 2 (2017) 5760–5768, <https://doi.org/10.1002/slct.201700963>.
- [9] M. Bhattu, D. Kathuria, B.K. Billing, M. Verma, Chromatographic techniques for the analysis of organophosphate pesticides with their extraction approach: A review (2015–2020), *Royal Society of Chemistry* 14 (4) (2022) 322–358.
- [10] B.o. Wang, Y. Li, H. Hu, W. Shu, L. Yang, J. Zhang, S.A. Zaidi, Acetylcholinesterase electrochemical biosensors with graphene-transition metal carbides nanocomposites modified for detection of organophosphate pesticides, *PLoS One.* 15 (4) (2020) e0231981.
- [11] M. Wang, Z. Li, Nano-composite ZrO₂/Au film electrode for voltammetric detection of parathion, *Sensors Actuators, B Chem.* 133 (2008) 607–612, <https://doi.org/10.1016/j.snb.2008.03.023>.
- [12] P.L. Chang, M.M. Hsieh, T.C. Chiu, Recent advances in the determination of pesticides in environmental samples by capillary electrophoresis, *Int. J. Environ. Res. Public Health.* 13 (2016) 409, <https://doi.org/10.3390/ijerph13040409>.
- [13] A.K. Malik, W. Faubel, A.K. Malik, W. Faubel, Critical Reviews in Analytical Chemistry A Review of Analysis of Pesticides Using Capillary A Review of Analysis of Pesticides Using Capillary Electrophoresis, *Crit. Rev. Anal. Chem.* 37–41 (2010).
- [14] P. Raghun, B.E. Kumara Swamy, T. Madhusudana Reddy, B.N. Chandrashekar, K. Reddaiah, Sol-gel immobilized biosensor for the detection of organophosphorous pesticides: A voltammetric method, *Bioelectrochemistry.* 83 (2012) 19–24, <https://doi.org/10.1016/j.bioelechem.2011.08.002>.
- [15] Y.H. Zheng, T.C. Hua, D.W. Sun, J.J. Xiao, F. Xu, F.F. Wang, Detection of dichlorvos residue by flow injection calorimetric biosensor based on immobilized chicken liver esterase, *J. Food Eng.* 74 (2006) 24–29, <https://doi.org/10.1016/j.jfoodeng.2005.02.009>.
- [16] A. Kumaran, R. Vashishth, S. Singh, S. U, A. James, P. Velayudhaperumal Chellam, Biosensors for detection of organophosphate pesticides: Current technologies and future directives, *Microchem. J.* 178 (2022), <https://doi.org/10.1016/j.microc.2022.107420>.
- [17] M. Bhattu, M. Verma, D. Kathuria, Recent Advancements in the Detection of Organophosphate Pesticides: A Review, *Anal. Methods.* 13 (2021) 4390–4428, <https://doi.org/10.1039/D1AY01186C>.
- [18] X. Xu, Y. Guo, X. Wang, W. Li, P. Qi, Z. Wang, X. Wang, S. Gunasekaran, Q. Wang, Sensitive detection of pesticides by a highly luminescent metal-organic framework, *Sensors Actuators B Chem.* 260 (2018) 339–345.
- [19] J. Yang, S.-W. Chen, B. Zhang, Q. Tu, J. Wang, M.-S. Yuan, Non-biological fluorescent chemosensors for pesticides detection, *Talanta.* 240 (2022) 123200.
- [20] Q. Chen, Y. Sun, S. Liu, J. Zhang, C. Zhang, H. Jiang, X. Han, L. He, S. Wang, K. Zhang, Colorimetric and fluorescent sensors for detection of nerve agents and organophosphorus pesticides, *Sensors Actuators B Chem.* 344 (2021), 130278.
- [21] R.J. Bushway, High-Performance Liquid Chromatographic Determination Of Trace Quantities Of Azinphos Methyl And Azinphos Methyl Oxon In Various Water Sources By Direct Injection And Trace Enrichment, *J. Liq. Chromatogr.* 5 (1982) 49–62, <https://doi.org/10.1080/01483918208068818>.
- [22] F. García Sánchez, A. Aguilar Gallardo, Spectrofluorimetric determination of the insecticide azinphos-methyl in cultivated soils following generation of a fluorophore by hydrolysis, *Analyst.* 117 (1992) 195–198, <https://doi.org/10.1039/AN9921700195>.
- [23] M.B. Kralj, P. Trebše, M. Franko, Oxidation as a pre-step in determination of organophosphorus compounds by the AChE-TLS bioassay, *Acta Chim. Slov.* 53 (2006) 43–51.
- [24] J. Tang, M. Zhang, G. Cheng, Y. Lu, Development of fluorescence polarization immunoassay for the detection of organophosphorus pesticides parathion and azinphos-methyl, *J. Immunoass. Immunochem.* 29 (2008) 356–369, <https://doi.org/10.1080/15321810802329757>.
- [25] B.H. Tangena, P.J.C.M. Janssen, G. Tiesjema, E.J. van den Brandhof, M. Klein Koerkamp, J.W. Verhoef, A. Filippi, W. van Delft, A Novel Approach for Early Warning of Drinking Water Contamination Events, *Water Contam. Emergencies Monit. Underst. Acting* (2011) 13–31, <https://doi.org/10.1039/9781849733199-00013>.
- [26] B. Liu, Y. Ge, Y. Zhang, Y. Song, Y. Chen, S. Wang, Development of a simplified enhanced chemiluminescence enzyme linked immunosorbent assay (ECL-ELISA) for the detection of phosmet, azinphos-methyl and azinphos-ethyl residues in vegetable samples, *Anal. Methods.* 5 (2013) 5938–5943, <https://doi.org/10.1039/c3ay40825f>.
- [27] A.M. Domínguez, F. Placencia, F. Cereceda, X. Fadic, W. Quiroz, Analysis of tomato matrix effect in pesticide residue quantification through QuEChERS and single quadrupole GC/MS, *Chil. J. Agric. Res.* 74 (2014) 148–156, <https://doi.org/10.4067/S0718-58392014000200004>.
- [28] T.T. Hu, C.M. Lu, H. Li, Z.X. Zhang, Y.H. Zhao, J. Li, Determination of Eleven organophosphorus pesticide residues in textiles by using HPLC-HRMS, *Anal. Sci.* 33 (2017) 1027–1032, <https://doi.org/10.2116/analsci.33.1027>.
- [29] R. Kaur, N. Kaur, A novel cation ensembled fluorescent organic nanoparticle for selective detection of organophosphorus insecticides, *Dye. Pigment.* 139 (2017) 310–317, <https://doi.org/10.1016/j.dyepig.2016.12.032>.
- [30] X. Wu, P. Wang, S. Hou, P. Wu, J. Xue, Fluorescence sensor for facile and visual detection of organophosphorus pesticides using AIE fluorogens-SiO₂-MnO₂ sandwich nanocomposites, *Talanta.* 198 (2019) 8–14, <https://doi.org/10.1016/j.talanta.2019.01.082>.
- [31] A.A. Wani, S.S. Chourasiya, D. Kathuria, P.V. Bharatam, 1,1-Diaminoazines as organocatalysts in phospho- Michael addition reactions, *Chem. Commun.* 57 (2021) 11717–11720, <https://doi.org/10.1055/sos-sd-042-00517>.
- [32] S.S. Chourasiya, D. Kathuria, A.A. Wani, P.V. Bharatam, Azines: Synthesis, structure, electronic structure and their applications, *Org. Biomol. Chem.* 17 (2019) 8486–8521, <https://doi.org/10.1039/c9ob01272a>.
- [33] D. Kathuria, S.S. Chourasiya, S.K. Mandal, A.K. Chakraborti, U. Beifuss, P. V. Bharatam, Ring-chain isomerism in conjugated guanilylhydrazones: Experimental and theoretical study, *Tetrahedron.* 74 (2018) 2857–2864, <https://doi.org/10.1016/j.tet.2018.04.042>.
- [34] D. Kathuria, S.S. Chourasiya, A.A. Wani, M. Singh, S.C. Sahoo, P.V. Bharatam, Geometrical Isomerism in Guanabenz Free Base: Synthesis, Characterization,

- Crystal Structure, and Theoretical Studies, *Cryst. Growth Des.* 19 (2019) 3183–3191, <https://doi.org/10.1021/acs.cgd.9b00026>.
- [35] G. Kumar, I. Singh, R. Goel, K. Paul, V. Luxami, *Spectrochimica Acta Part A : Molecular and Biomolecular Spectroscopy* Dual-channel ratiometric recognition of Al³⁺ and F⁻ ions through an ESIPT-ESICT signalling mechanism, *Spectrochim. Acta Part A Mol. Biomol. Spectrosc.* 247 (2021), 119112, <https://doi.org/10.1016/j.saa.2020.119112>.
- [36] Y. Zhang, L. Zhang, *Spectrochimica Acta Part A : Molecular and Biomolecular Spectroscopy* A novel “turn-on” fluorescent probe based on hydroxy functionalized naphthalimide as a logic platform for visual recognition of H₂S in environment and living cells, *Spectrochim. Acta Part A Mol. Biomol. Spectrosc.* 235 (2020), 118331, <https://doi.org/10.1016/j.saa.2020.118331>.
- [37] L. Ji, C. Yang, H. Li, N. Yang, Y. Fu, L. Yang, Q. Wang, G. He, A reactive probe for Co²⁺ ion detection based on a catalytic decomposition process and its fluorescence imaging in living cells, *Luminescence.* 36 (2021) 4–10, <https://doi.org/10.1002/bio.3909>.
- [38] R. Suhasini, R. Karpagam, K. Thirumoorthy, V. Thiagarajan, “Turn-on” unsymmetrical azine based fluorophore for the selective detection of diethylchlorophosphate via photoinduced electron transfer to intramolecular charge transfer pathway, *Spectrochim. Acta - Part A Mol Biomol. Spectrosc.* 263 (2021), 120206, <https://doi.org/10.1016/j.saa.2021.120206>.
- [39] M. Verma, A. Kaur, H. Kaur, N. Kaur, Selective Determination of Silver Metal Ion Using Polyamine-Based Ratiometric Chemosensor in an Aqueous Medium and Its Real-Time Applicability as a Silver Sink, (2018) 7792–7799. <https://doi.org/10.1002/slct.201702540>.
- [40] M. Chaudhary, M. Verma, K.C. Jena, N. Singh, Histidine-Naphthalimide based Organic-Inorganic Nanohybrid for Electrochemical Detection of Cyanide and Iodide ions, *ChemistrySelect.* 5 (2020) 8246–8252, <https://doi.org/10.1002/slct.202001968>.
- [41] J. Singh, S. Kaur, J. Lee, A. Mehta, S. Kumar, K.-H. Kim, S. Basu, M. Rawat, Highly fluorescent carbon dots derived from *Mangifera indica* leaves for selective detection of metal ions, *Sci. Total Environ.* 720 (2020), 137604.
- [42] V. Thiagarajan, P. Ramamurthy, D. Thirumalai, V.T. Ramakrishnan, A novel colorimetric and fluorescent chemosensor for anions involving PET and ICT pathways, *Org. Lett.* 7 (4) (2005) 657–660.
- [43] V. Thiagarajan, P. Ramamurthy, Specific optical signalling of anions via intramolecular charge transfer pathway based on acridinedione fluorophore, *J. Lumin.* 126 (2) (2007) 886–892.
- [44] M.J. Frisch, G.W. Trucks, H.B. Schlegel, G.E. Scuseria, M.A. Robb, J.R. Cheeseman, G. Scalmani, V. Barone, G.A. Petersson, H. Nakatsuji, *Gaussian 16* (2016).
- [45] R.G. Parr, W. Yang Density functional theory of atoms and molecules, Oxford Univ. Press. 1 (1989) 1989.